



DE87013506

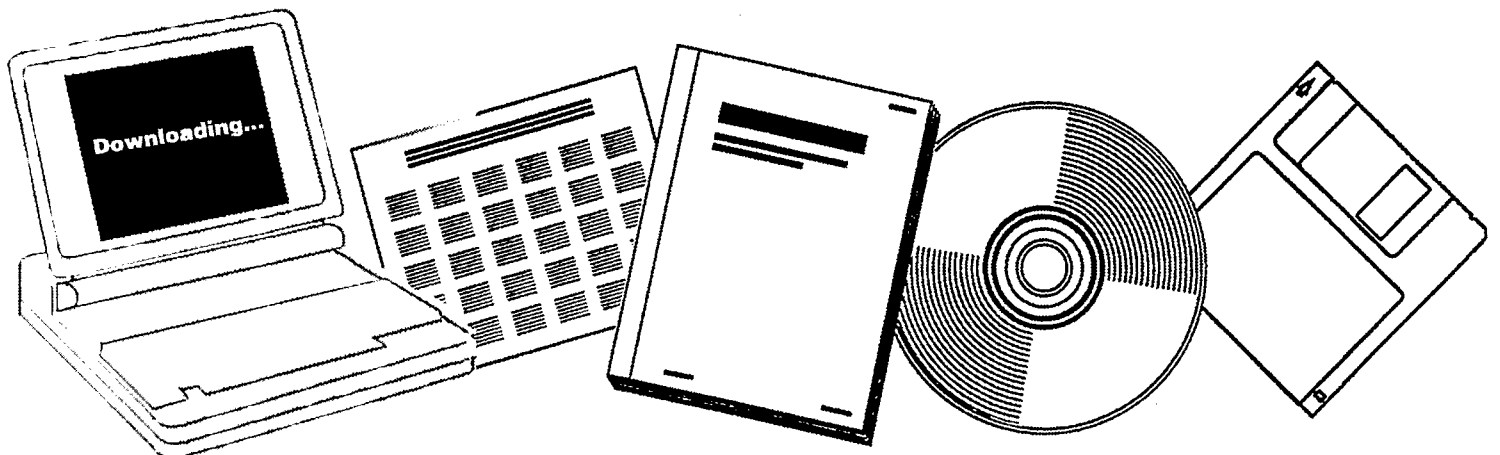
NTIS

One Source. One Search. One Solution.

**NOVEL EXPERIMENTAL STUDIES FOR COAL
LIQUEFACTION: QUARTERLY PROGRESS REPORT,
APRIL 1, 1987 TO JUNE 30, 1987**

PITTSBURGH UNIV., PA

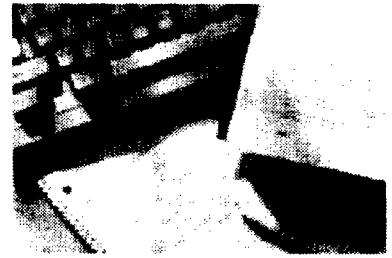
1987



U.S. Department of Commerce
National Technical Information Service

One Source. One Search. One Solution.

NTIS



Providing Permanent, Easy Access to U.S. Government Information

National Technical Information Service is the nation's largest repository and disseminator of government-initiated scientific, technical, engineering, and related business information. The NTIS collection includes almost 3,000,000 information products in a variety of formats: electronic download, online access, CD-ROM, magnetic tape, diskette, multimedia, microfiche and paper.



Search the NTIS Database from 1990 forward

NTIS has upgraded its bibliographic database system and has made all entries since 1990 searchable on **www.ntis.gov**. You now have access to information on more than 600,000 government research information products from this web site.

Link to Full Text Documents at Government Web Sites

Because many Government agencies have their most recent reports available on their own web site, we have added links directly to these reports. When available, you will see a link on the right side of the bibliographic screen.

Download Publications (1997 - Present)

NTIS can now provides the full text of reports as downloadable PDF files. This means that when an agency stops maintaining a report on the web, NTIS will offer a downloadable version. There is a nominal fee for each download for most publications.

For more information visit our website:

www.ntis.gov



U.S. DEPARTMENT OF COMMERCE
Technology Administration
National Technical Information Service
Springfield, VA 22161



LEGIBILITY NOTICE

A major purpose of the Technical Information Center is to provide the broadest dissemination possible of information contained in DOE's Research and Development Reports to business, industry, the academic community, and federal, state and local governments.

Although a small portion of this report is not reproducible, it is being made available to expedite the availability of information on the research discussed herein.

DOE/PC/71257-T11

DE87013506



DOE/PC/71257--T11

DE87 013506

Quarterly Progress Report

NOVEL EXPERIMENTAL STUDIES
FOR COAL LIQUEFACTION

Gerald D. Holder
Yatish T. Shah
John W. Tierney

University of Pittsburgh
Pittsburgh, PA 15261

Prepared for the Department of Energy
Contract No. DE-FG22-84PC71257

April 1, 1987 to June 30, 1987

DISCLAIMER

This report was prepared as an account of work sponsored by an agency of the United States Government. Neither the United States Government nor any agency thereof, nor any of their employees, makes any warranty, express or implied, or assumes any legal liability or responsibility for the accuracy, completeness, or usefulness of any information, apparatus, product, or process disclosed, or represents that its use would not infringe privately owned rights. Reference herein to any specific commercial product, process, or service by trade name, trademark, manufacturer, or otherwise does not necessarily constitute or imply its endorsement, recommendation, or favoring by the United States Government or any agency thereof. The views and opinions of authors expressed herein do not necessarily state or reflect those of the United States Government or any agency thereof.

MASTER

DISTRIBUTION OF THIS DOCUMENT IS UNLIMITED

NOVEL EXPERIMENTAL STUDIES FOR COAL LIQUEFACTION

Research is being carried out in this project in two areas which are of interest to ongoing investigations at the Pittsburgh Energy Technology Center (PETC). They are: (a) thermal behavior of slurry reactors used for indirect coal liquefaction, and (b) coal liquefaction under supercritical conditions. The current status of each of these tasks is summarized in this report.

TASK I:

Scope of Work

In Task I of this project, the use of a slurry reactor for indirect coal liquefaction is being studied. Work is being done using three indirect liquefaction routes involving synthesis gas -- the Fisher-Tropsch reaction, the one-step conversion to methanol, and the two-step conversion to methanol via methyl formate.

Results and Highlights

Experimental work and data analysis for the two-step methanol synthesis in a single slurry reactor were continued during the quarter. Experimental work included the effect of the H_2/CO ratio on the simultaneous reactions and measurements of the solubility of hydrogen and CO in methanol and methyl formate. Reaction rates obtained experimentally for the simultaneous system were compared with rates calculated from the individual reactions.

Effect of H_2/CO on Reaction Rate

The two-step methanol synthesis involves two reactions, and one of the reactants in each reaction is a gas. The carbonylation of methanol requires CO and the hydrogenolysis of methyl formate requires H_2 . The ratio of H_2 to CO is therefore a very important operating parameter, affecting the relative rates of the two reactions and the total methanol production rate. It may also affect the selectivity of the two reactions.

Two runs were made, one at a temperature of $121^\circ C$ and the other at $140^\circ C$. All reaction conditions were constant except for the H_2/CO ratio. The experimental procedure was the same as described in previous reports, and

important operating conditions are listed in Table 1-1. During each run the ratio was changed in a random order to confound the effect of reactant ratio and catalyst aging, and an average of 8 hours was used for each measurement.

TABLE 1-1
Operating Conditions for Runs
to Determine Effect of H₂/CO Ratio

Run #	T (C)	P (psig)	CH ₃ OK (g)	G-89 (g)	Feed Gas Flow Rate (cc/min)
1	121	930	5	15	330
2	140	900	15	20	330

The reaction rates are shown in Figure 1-1 and are corrected for catalyst aging. The maximum correction was 6%. The slopes at each run are essentially the same and indicate that higher methanol production was obtained at lower H₂/CO ratio. This result was unexpected. In the quarterly report for October-December 1986, it was shown that by assuming the simultaneous reaction kinetic expression could be obtained by combining the kinetic expressions for the individual reactions as follows:

$$Y_{\text{meoh}} = \frac{4.49 \times 10^{-7} \exp\left(-\frac{1686}{T}\right) C_{\text{catal},2} C_{\text{MeOH}} P_{\text{CO}} P_{\text{H}_2}}{1 + 0.096 P_{\text{CO}}} \quad (1)$$

At the operating conditions used, it can be shown that the optimal H₂/CO ratio should be 2.5 if the equation applies. The fact that the observed optimal rate is

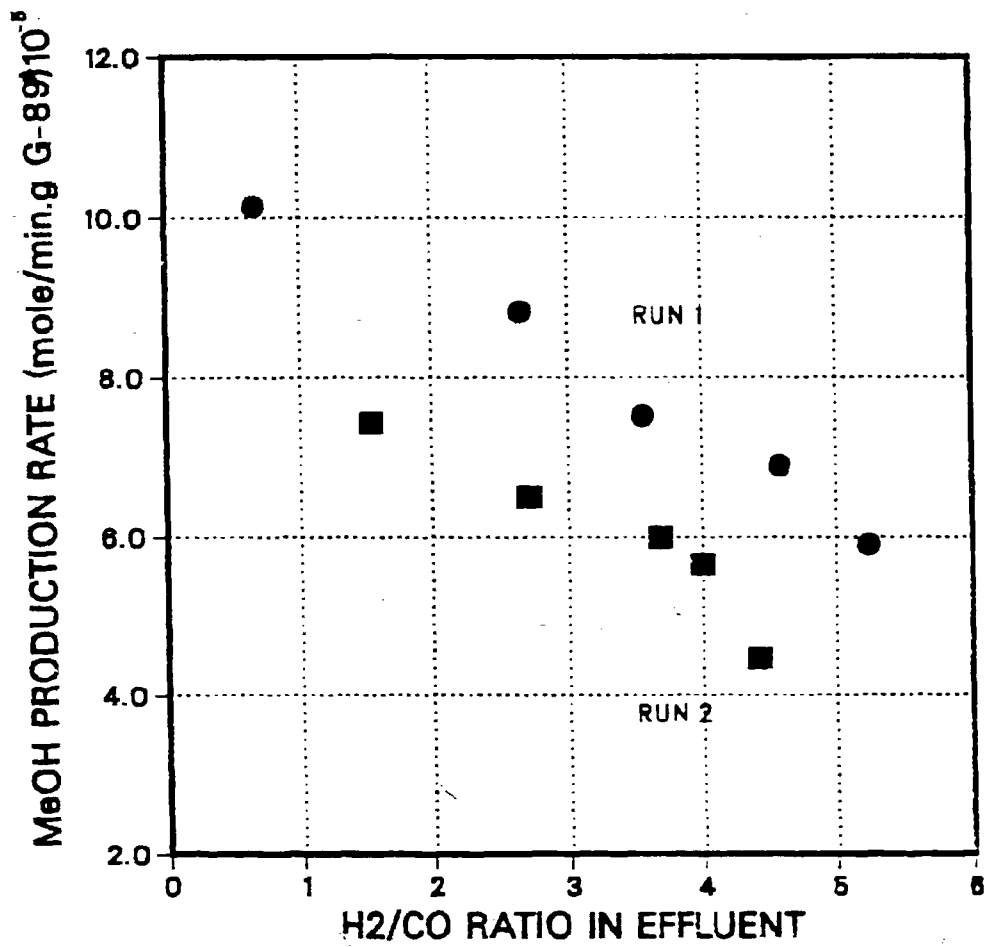


Figure 1-1: Effect of H₂/CO Ratio

much lower implies that the equation must be modified when the two reactions are carried out simultaneously.

Further evidence that there is an interaction between the two reactions is shown in Figure 1-2. This shows the measured rate for the simultaneous reaction divided by the calculated rate from the hydrogenolysis rate equation (equation 2 in the quarterly report for October-December 1986) at the same conditions plotted versus time. At time zero, before any aging effect has taken place, the rate is approximately twice the calculated rate at 140°C, 1.6 times the calculated rate at 160°C and 0.8 times the calculated rate at 180°C. It appears that there is a synergistic effect when the two reactions take place simultaneously at 140°C and 160°C. Work is continuing to analyze these data.

Solubility Measurements

Solubility measurements were made for CO and H₂ in both pure methanol and pure methyl formate. The data are needed because the reaction takes place in the liquid phase, and liquid concentrations are needed to properly correlate the data for changing liquid composition. The data for the individual reactions were largely taken for essentially pure methanol (carbonylation) or for essentially pure formate (hydrogenolysis).

The solubilities were measured by a batch absorption technique similar to that used by Shah (1). The liquid was degassed and then heated to the experimental temperature. With the stirrer off, gas was added until the desired pressure was reached. The stirrer was then turned on, and the decrease in pressure noted after the system came to equilibrium.

The solubilities are related to the partial pressures in the gas phase by the fact that the fugacity in liquid and vapor must be the same

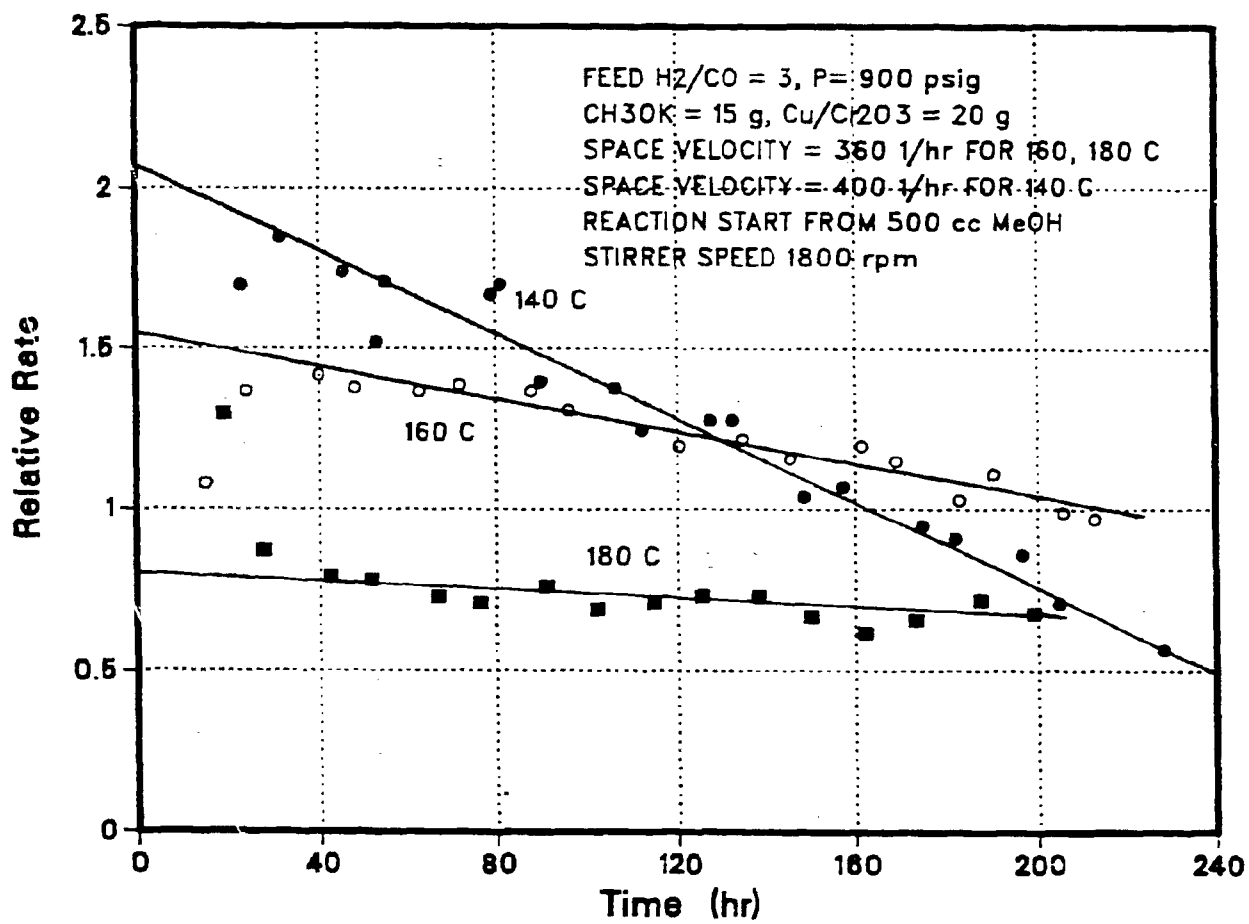


FIGURE 1-2: Comparison of Hydrogenolysis Rate in Simultaneous Operation and Individual Operation

$$f_i = \phi_i y_i P = H_{i,\text{solvent}} x_i$$

where ϕ_i and y_i are the fugacity coefficient and mole fraction at component i in the gas phase, x_i is the mole fraction of component i in the liquid phase. $H_{i,\text{solvent}}$ is the Henry's constant of solute i in the solvent. P is the total pressure. This can be solved for Henry's constant, to give

$$H_{i,\text{solvent}} = \frac{\phi_i y_i P}{x_i}$$

The total gas pressure was known and was corrected for the partial pressure of methanol or methyl formate, giving the partial pressure of either CO or H₂. The liquid composition was calculated from the change of pressure after the stirrer was turned on. The fugacity coefficient in the vapor was calculated from the virial equation of state (2). At least three data points were taken at each temperature, and the average values used. At least three temperatures were used for each of the four binary pairs. A plot of Henry's constant versus temperature is shown in Figures 1-3 and 1-4. These results were then correlated using

$$\ln H_{i,\text{solvent}} = A + B/T, \quad B = \frac{\Delta h}{R}$$

where A and B are constants, Δh is enthalpy of solution, R is the gas constant.

The results of the correlation are shown in Table 1-2. The correlation coefficient, r , and temperature range used are also given.

TABLE 1-2

Coefficients to be Used in Equations for Henry's Law Parameter

$$H_{i,\text{solvent}} = A + B/T$$

System	A	B	Δh (kJ/mole)	r	Temperature Range (C)
CO-MeOH	3.07	1993	16.57	.94	120,140,160,180
CO-MeF	2.92	1721	14.31	.97	120,140,180
H ₂ MeOH	3.66	1909	15.87	.99	120,140,160,180
H ₂ -MeF	2.14	2314	19.24	.98	120,140,160,180

Future Work

During the next quarter, analysis of the data obtained for the simultaneous conversion of syngas to methanol via methyl formate will be continued. In addition, work will be continued on the measurement of thermal effects associated with the Fischer-Tropsch synthesis in a slurry reactor.

References

1. R.S. Albal, Y.T. Shah, A. Schumpe, and N.L. Carr, The Chemical Engineering Journal, 27 (1983), 61-80.
2. J.M. Smith and H.C. Van Ness, "Introduction to Chemical Engineering Thermodynamics," Third Edition, McGraw-Hill, Inc., 1975.

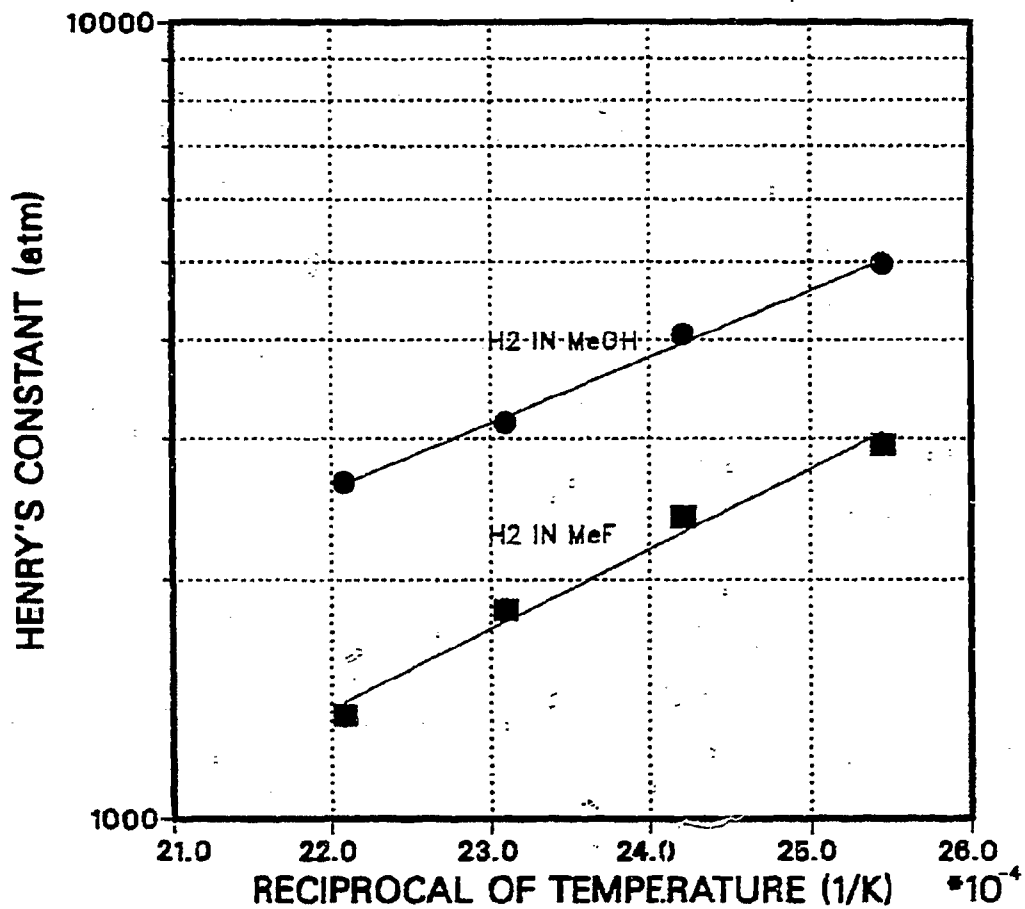


FIGURE 1-3: Dependence of Henry's Constant of Hydrogen in Merhanol and Methyl Formate on Temperature

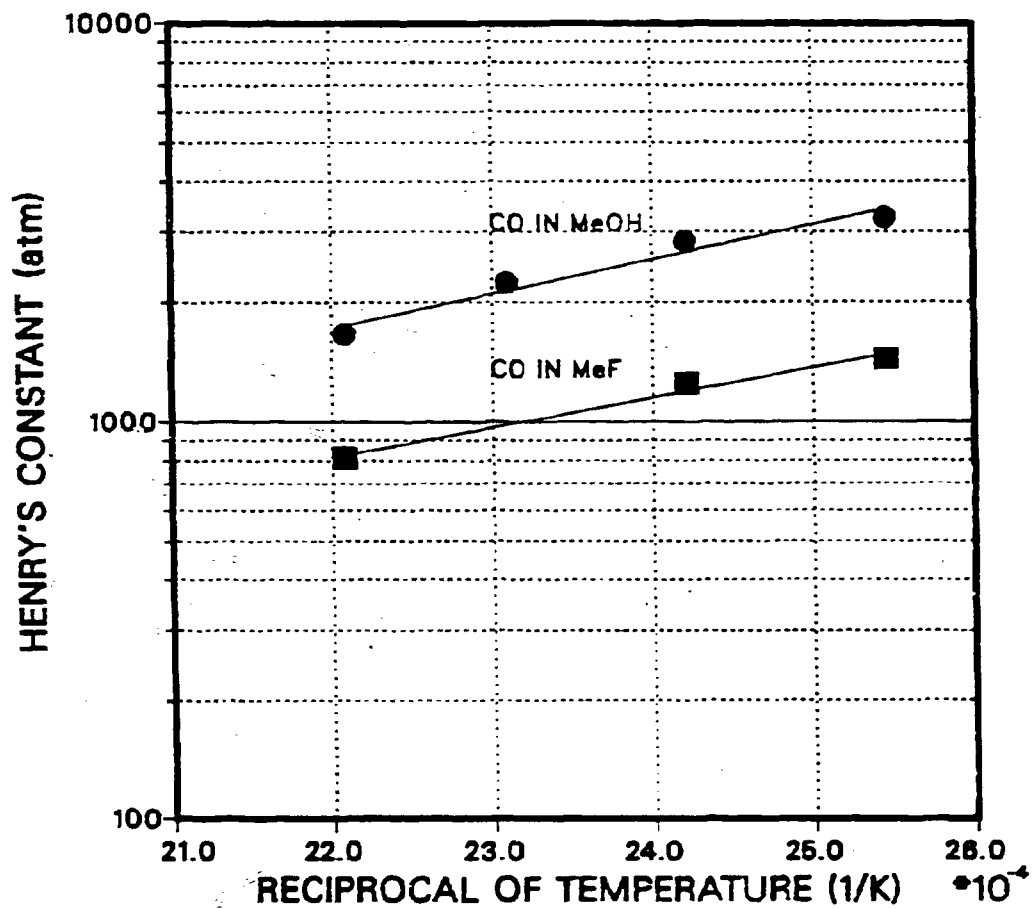


FIGURE 1-4: Dependence of Henry's Constant of CO in Methanol and Methyl Formate on Temperature

TASK 2: COAL LIQUEFACTION UNDER SUPERCRITICAL CONDITIONS

Supercritical fluid extraction is an attractive process primarily because the density and solvent power of a fluid changes dramatically with pressure at near critical conditions, and during the extraction of coal, the density of a supercritical fluid should also change the extractability of the coal. During earlier quarters a non-reacting supercritical fluid, toluene, was studied to determine the effect of density on the coal extraction/reaction process. Extractions were carried out for 2 to 60 minutes at reduced densities between 0.5 and 2.0 and at temperatures between 647 and 698 K. The data obtained can be explained by the hypothesis that coal dissolution is required preceding liquefaction reactions and that the degree of dissolution depends upon solvent density and temperature. A kinetic model shows that higher solvent densities result in faster conversion rates and in higher total conversions. Two papers have resulted from this study.

A second factor that makes supercritical extraction attractive is high mass transfer rates. At high pressures, mass transfer rates in a supercritical fluid are much higher than in a liquid, despite the fact that the supercritical fluid has liquid-like solvent powers. The objective of this work is to measure mass transfer rates for naphthalene extraction by carbon dioxide to enable us to determine how mass transfer coefficients vary with pressure, flow rate, and bed height, since these parameters will influence the design of extraction or reaction processes which utilize supercritical fluids. Ultimately, such measurements will be extended to coal/supercritical fluid systems to help define the flow rates liquid/solvent ratios that would be appropriate for a supercritical system.

In this report, the entire program for evaluating mass transfer coefficients under supercritical conditions is described and a review of current knowledge and planned correlational approaches is given.

BACKGROUND

Historically, interest in supercritical fluids was initially related to the observation that such fluids were often excellent solvents. This fact was discovered over 100 years ago by Hannay¹² and by Hannay and Hogarth.^{13,14} Prior to that time, it was generally thought that materials above their critical temperatures would be gaseous in nature and thus poor solvents.

Studies of solubilities in supercritical fluids have been continued^{15,16} and in most instances, they concentrated on developing phase diagrams for binary mixtures, particularly pressure-temperature projections. Vapor-liquid equilibrium data on binary hydrocarbon systems at elevated pressure became available in the 1930's^{17,18} and the first patent for the practical application of supercritical extraction was made in 1943.¹⁹ Later, Maddacks,²⁰ Tugrul²¹ and Bartle et al.²² described the extraction of components of low volatility from coal liquids using supercritical toluene. Barton and Fenske²³ suggested using C₁₁ and C₁₂ paraffinic fractions to desalinate sea water. Hubert and Vitzhu²⁴ studied on the removal of nicotine from tobacco leaves, of caffeine from green coffee beans, and the separation of a hop extract from commercial hops, in all cases using supercritical carbon dioxide. Modell et al.^{25,26} discussed the regeneration of activated carbon by the use of supercritical carbon dioxide.

Critical data for a number of possible supercritical fluid solvents are listed in Table 2-1. These gases are suitable as a solvent either on their own or as components of mixtures. Because of their low critical temperatures, several of them can be used to extract heat-labile substances. Particularly, supercritical carbon dioxide is a very attractive solvent for practical applications because it is nonflammable, nontoxic, environmentally acceptable and relatively inexpensive. The critical temperature of carbon dioxide is only 304°K (31°C) and thus it can be used at moderate temperature for the extraction of heat sensitive substances

without degradation. One good example of using supercritical carbon dioxide is shown in selective extraction of caffeine from green coffee beans.

Table 2-1: Critical Data for Some Supercritical Solvents⁷⁹

Substance	Critical Temperature K	Critical Pressure MPa	Critical Density g cm ⁻³
Methane	191	4.60	0.162
Ethylene	282	5.03	0.218
Chlorotrifluoro methane	302	3.92	0.579
Carbon dioxide	304	7.38	0.468
Ethane	305	4.88	0.203
Propylene	365	4.62	0.233
Propane	370	4.24	0.217
Ammonia	406	11.3	0.235
Diethyl ether	467	3.64	0.265
n. Pentane	470	3.37	0.237
Acetone	508	4.70	0.278
Methanol	513	8.09	0.272
Benzene	562	4.89	0.302
Toluene	592	4.11	0.292
Pyridine	620	5.63	0.312
Water	647	22.0	0.322

The supercritical fluid (SCF) region is not defined rigorously, but for the practical considerations, the SCF region is usually defined at conditions bounded approximately by $0.9 < T_r < 1.2$ and $P_r > 1.0$ where the SCF is very compressible as illustrated in Figure 2-1. For example, at a constant T_r of 1.0, increasing pressure from $P_r = 0.8$ to $P_r = 1.2$ significantly increases the density from gas-like densities to liquid-like densities. At higher reduced temperature, the pressure increase required to increase an equivalent density becomes greater. This practical consideration sets the upper bound on temperature. At higher pressures, the density is less sensitive to temperature changes. In the vicinity of the critical

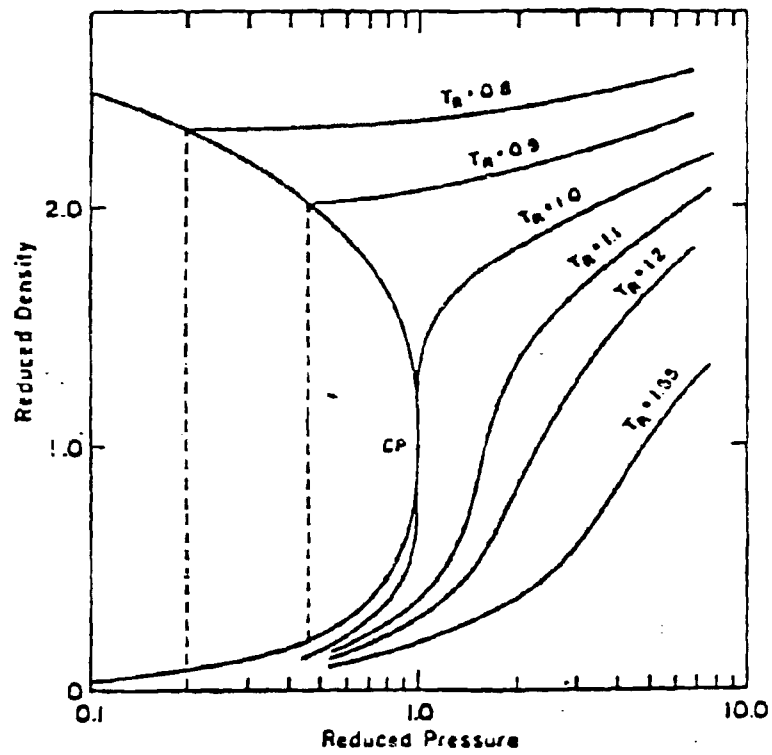


Figure 2-1: Reduced density-reduced pressure diagram for carbon dioxide at various reduced temperatures (T_r) in the vicinity of the critical point (CP) ³⁵

point, large density changes can be obtained with either relatively small pressure or temperature changes.

The effect of SCF solvent density on solubilities is shown directly in Figure 2-2 in the naphthalene-ethylene system.^{27,28} Solubilities increase with increasing ethylene densities along each isotherm due to increasing solvent power, and with increasing temperature at constant density due to increasing volatility of naphthalene. These solvent properties vary continuously with solvent density and thus control solvent power and enhance the selectivity of the solvent. Also solvent and solute can be easily separated, and we can fractionate multiple solutes by stepwise reductions in solvent density.

In addition, SCF have better physicochemical properties than do gases and liquids. The order-of-magnitude comparison shown in Table 2-2 indicates that, while SCF has liquid-like densities, its viscosities and diffusivities are intermediate to those properties for liquids and gases. Thus SCF has the solvent power of liquids with better mass-transfer properties.

Table 2-2: Order of Magnitude Comparison of Gas, SCF and Liquid Phases³⁵

<u>Property</u>	<u>Gas</u>	<u>Phase SCF*</u>	<u>Liquid</u>
Density (kg/m ³)	1	700	1000
Viscosity (Ns/M ²)	10 ⁻⁵	10 ⁻⁴	10 ⁻³
Diffusion coefficient (cm ² /s)	10 ⁻¹	10 ⁻⁴	10 ⁻⁵

* At $T_r = 1$ and $P_r = 2$

** 10^3 centipoise = 1 Ns/m²

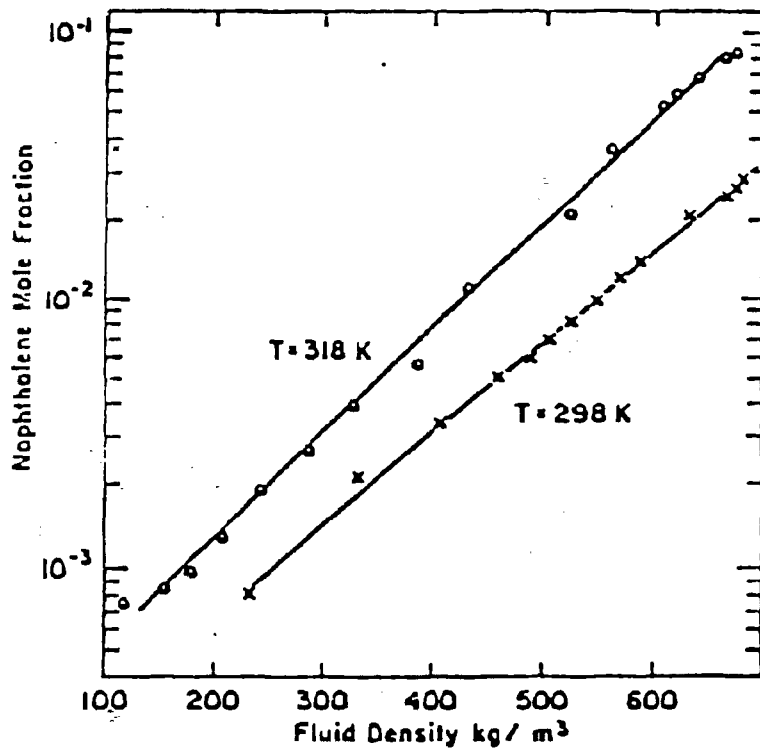


Figure 2-2: Solid solubilities of naphthalene in compressed ethylene as a function of ethylene density ³⁵

DIFFUSION COEFFICIENT AND VISCOSITY

The development of mass-transfer models requires knowledge of the diffusion coefficient of the solute, the viscosity, and the density of the fluid phase which can be used to correlate mass transfer coefficients.

Experimental data on diffusion coefficients in supercritical condition are scarce. Most studies on diffusion coefficient in the high pressure had been limited to the measurement of self diffusion coefficients, and binary diffusion coefficients in simple systems such as H_2-N_2 , $He-N_2$ and H_2-Ar .³² But recently, several experiments has been done to measure the diffusivities in systems such as naphthalene- CO_2 ,^{33,34} benzene- CO_2 and caffeine- CO_2 .³³ As a result of this work, it has been found that the viscosities and diffusivities of supercritical fluids were strongly dependent upon pressure and temperature in the vicinity of the critical point, and the ratios $(D_{VP})/(D_{VP})^0$ were 0.8 to 1.2. $(D_{VP})^0$ is the value calculated on the basis of the low density theory for a gas at the given temperature. In the recent review article,³⁵ diffusion coefficient for the several systems were shown as a function of reduced pressure in Figure 2-3.

The viscosity of compressed fluids have been studied quite extensively. In Figure 2-4, the typical data of the viscosities of supercritical carbon dioxide is given as a function of pressure.³⁶ At the low pressure, the viscosities of carbon dioxide are essentially independent of pressure, but above the critical pressure, the viscosities increase rapidly with pressure.

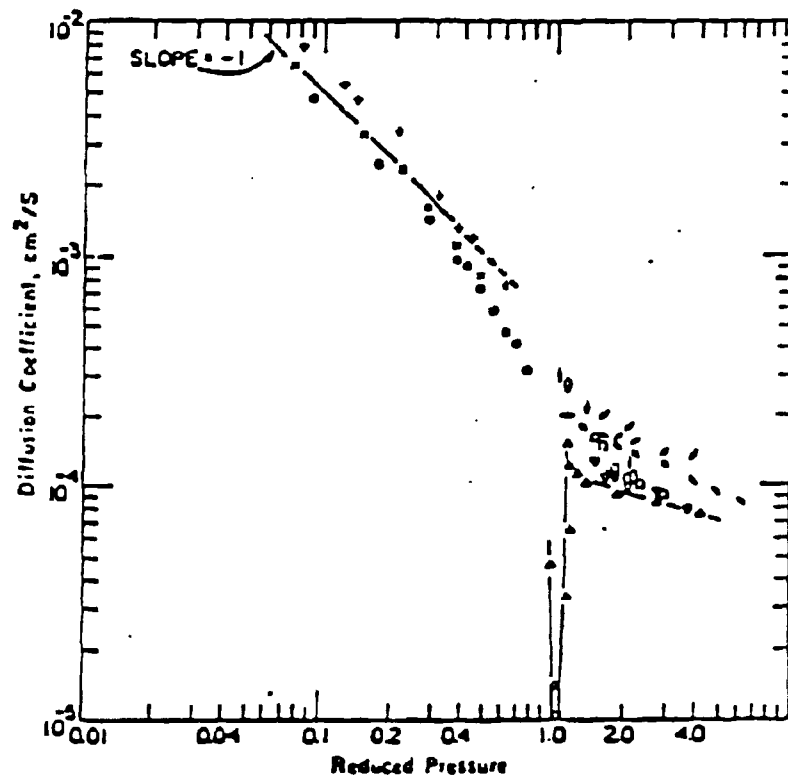


Figure 2-3: Diffusion coefficient in supercritical fluids ³⁵

Table 2-3: Key for figure 2-3.

Symbol	T, °C	System	Reference
.	20	CO ₂ -Naphthalene	56, 57
x	30		
+	40		
△	35	CO ₂ -Naphthalene	58
▽	55		
/	12	Ethylene-Naphthalene	58
\	35		
- - -	40	CO ₂ -Benzene	60
	40	CO ₂ -Propylbenzene	34
o	40	CO ₂ -1,2,3-Trimethylbenzene	34

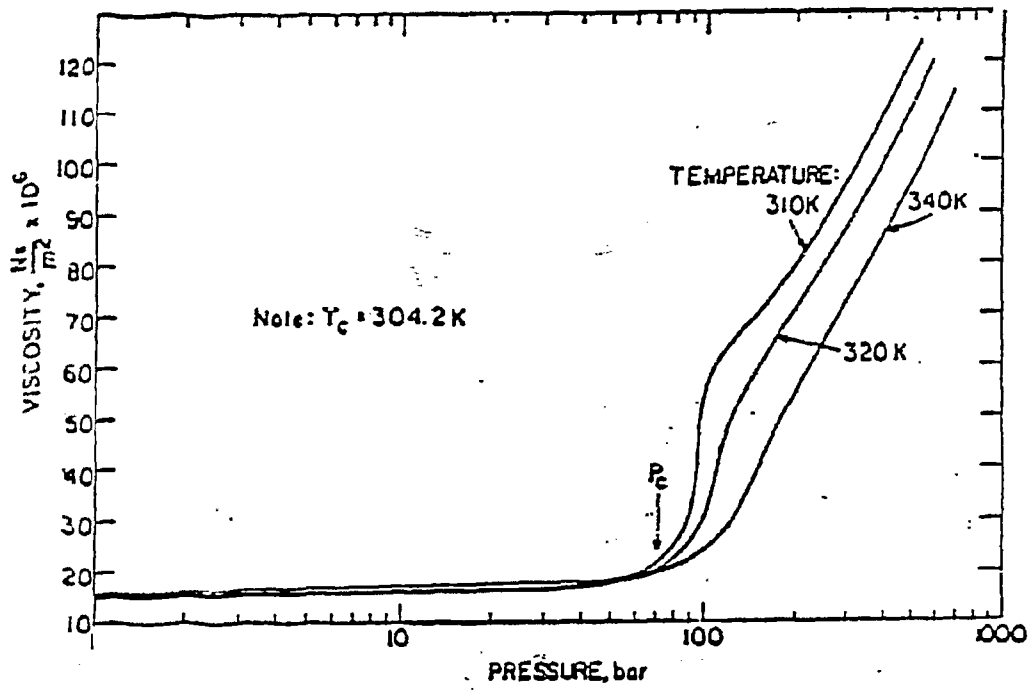


Figure 2-4: Viscosity of supercritical carbon dioxide³⁵

MODELS FOR FLOW SYSTEM IN A PACKED BED

The packed bed reactor is applicable in many operations, such as extraction, adsorption, leaching, ion exchange and catalytic processes. Therefore, mass-transfer coefficients in packed beds is the focus of the current research. First models for determining mass transfer from our experiments (past 38) will be developed and then these coefficients will be correlated.

The simplest flow model for the packed bed is the ideal plug flow model with no longitudinal mixing but complete radial mixing. Although no actual reactors can be fully represented by an ideal model, the plug flow model can be used in a number of packed bed reactors which behave close to the ideal.

However, flow behavior of most of the actual packed bed reactors deviates from ideal conditions. The deviation may be caused by nonuniform velocity profile, velocity fluctuation due to molecular or turbulent diffusion, by short-circuiting, by-passing and channeling of fluid, and by the presence of stagnant regions of fluid caused by the reactor shape and internals. Many flow models considering the nonideality of the flow pattern in packed reactor have been proposed.³⁷⁻⁴¹ Among them, the cell model or compartment model^{40,41} is one of the most widely used models owing to its advantages over other models as described below. We used these two models (ideal plug flow model and cell model) to get mass-transfer coefficients and estimate nonideality.

The Ideal Plug Flow Model

Flow patterns in packed bed reactors with small ratios of the tube and particle diameter to length can be closely approximated by plug flow. The measurement of mass-transfer coefficients is based upon the following equation:

$$dN_A = d(V_T y_A) = k_y (y_A^* - y_A) dA = k_y (y_A^* - y_A) a_S S dL \quad (2-1)$$

Here,

$$V_T = \frac{1'}{1 - y_A} \quad (2-2)$$

where V' is molal flow rate of inert component in moles per unit time. Therefore,

$$d(V_T y_A) = V' d\left(\frac{y_A}{1 - y_A}\right) = v' \frac{dy_A}{(1 - y_A)^2} = V_T \frac{dy_A}{(1 - y_A)} \quad (2-3)$$

From equations (2-1) and (2-2)

$$\int_{y_{A, \text{in}}=0}^{y_{A, \text{out}}} \frac{dy_A}{(1 - y_A)(y_A^* - y_A)} = \frac{k_y a_S}{\bar{G}_{My}} \int_0^{L_T} dL \quad (2-4)$$

where \bar{G}_{My} is the average molal mass velocity of the gas in moles per unit area per unit time. For dilute gas (i.e., $1 - y_A = 1$),

$$\int_0^{y_{A, \text{out}}} \frac{dy_A}{y_A^* - y_A} = \left(\frac{k_y a_S}{\bar{G}_{My}}\right) L_T \quad (2-5)$$

By integration and rearrangement,

$$k_{y a S} = \left(\frac{G_M y}{L_T} \right) \ln \left(\frac{y_A^*}{y_A - y_{A, out}} \right)$$

Axial Dispersion in a Packed Bed

Several models have been used to analyze and correlate experimental data on mixing in a packed bed. They introduced radial and/or axial diffusion coefficients E_r and/or E_a , independent of solute concentration, to take into account the mixing effect in the radial and/or axial directions respectively, for packed beds. These diffusion coefficients can be related to flow parameters, fluid properties and the geometry of the bed and the packing.

In a packed bed catalytic reactor, a chemical reaction takes place in a bed and heat flows through the tube wall and therefore, the radial heat and mass transfer are not negligible. However, radial dispersion can usually be neglected compared with axial dispersion when the ratio of column diameter to length is small and the flow is in the turbulent regime. Many investigators have found that the mixing effect in packed beds could be well described in an axial dispersion coefficient E_a alone even though there was some radial dispersion effect.

Dankwerts⁴¹ first published the results on axial dispersion in a packed bed. Wen and Fan⁴² summarized the results of previous investigations on the axial dispersion of liquids (Figure 2-5) and gases (Figure 2-6) in packed beds and have developed empirical correlations (shown below) based on about 500 data points for liquids and gases, respectively. The axial Peclet number Pe_a is defined as $d_p u / E_a$. These equations can be used to determine the axial diffusion coefficient E_a for liquids and gases, respectively.

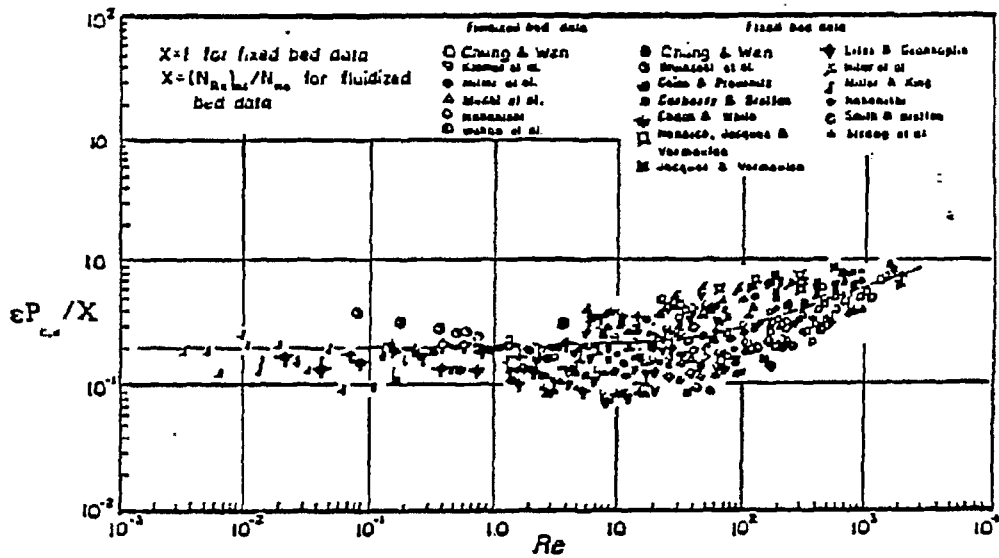


Figure 2-5: A Correlation of longitudinal dispersion coefficient of liquid phase fixed beds and fluidized beds in terms of peclt number

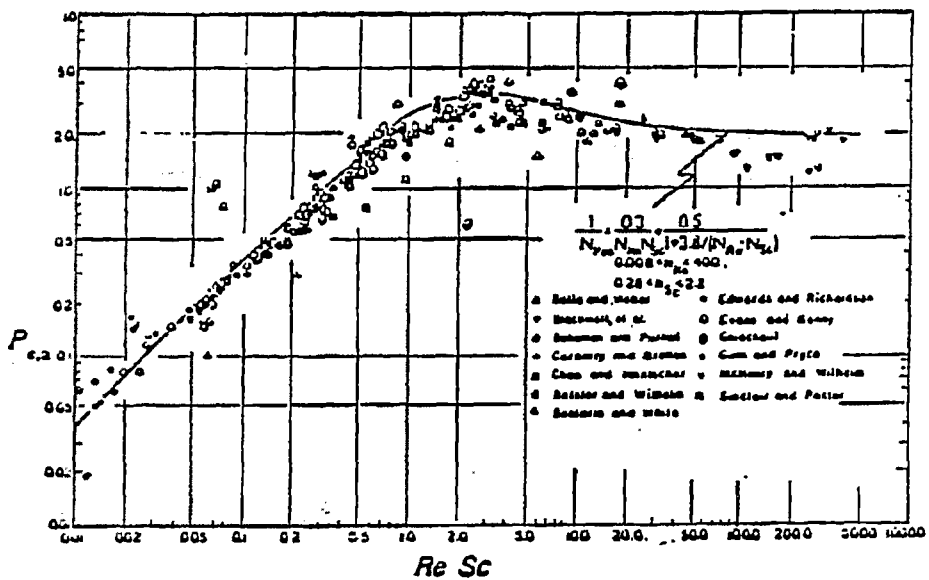


Figure 2-6: Correlation of axial dispersion coefficient for gases flowing through fixed beds

Liquids:

$$\epsilon P_{e,a} = 0.2 + 0.11 \text{ Re}^{0.48} \quad (2-7)$$

Gases:

$$\frac{1}{P_{e,a}} = \frac{0.3}{\text{ScRe}} + \frac{0.5}{1 + 3.8(\text{ReSc})^{-1}} \quad (2-8)$$

for $0.008 < \text{Re} < 400$ and $0.28 < \text{Sc} < 2.2$

The general correlation of existing data of the axial dispersion coefficient for liquids and gases respectively⁴³ is shown in Figure 2-7. The dashed lines represent the molecular-diffusion asymptotes, for $Pe = (\text{Re})(\text{Sc})T_c/\epsilon$. The lines shown are for $T_c = \sqrt{2}$ and $\epsilon = 0.4$. In the case of gases, $P_{e,a}$ remains approximately constant,

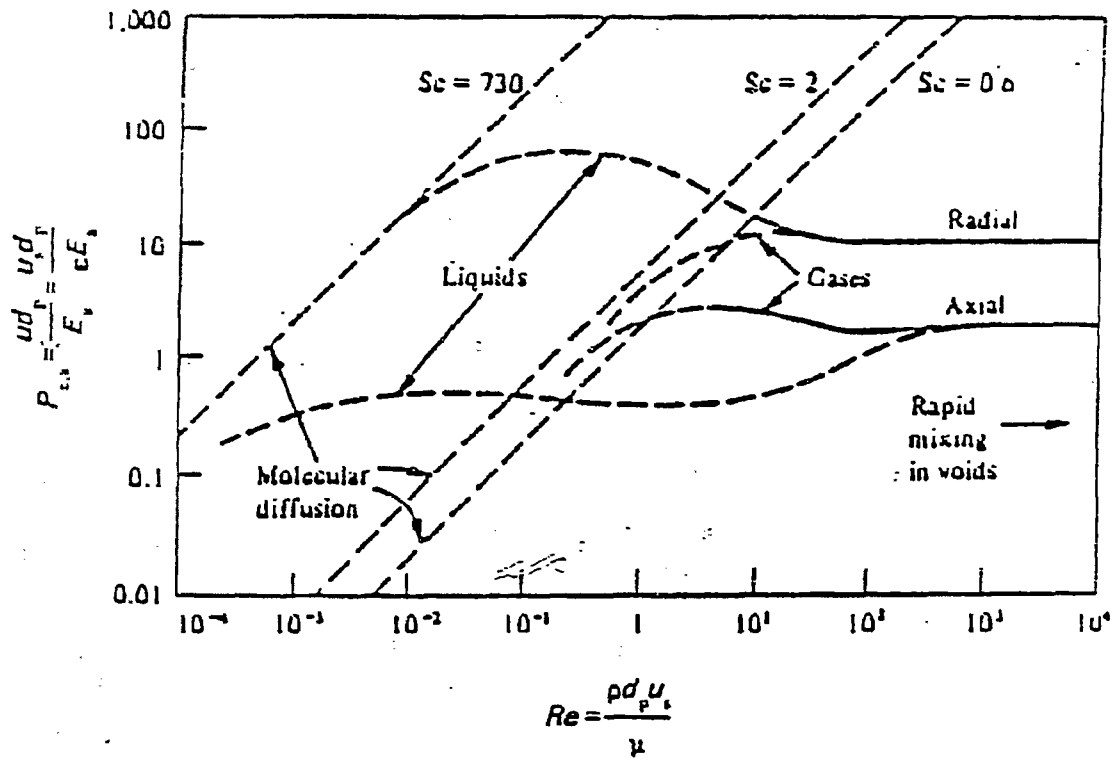


Figure 2-7: Approximate representation of a large amount of published data on radial and axial dispersion in randomly packed beds of uniform spheres: flow of a single phase ⁴³

decreasing little from its value of 2 until molecular diffusion is important at Re around 1.0. Molecular diffusion in liquids, however, is so slow that E_a increases as Re is reduced below 500. But as Re is decreased from 300 to 10, $P_{e,a}$ remains approximately proportional to Re indicating that E_a is roughly constant in this region. The correction of $P_{e,a}$ with Re is greatly dependent on the magnitude of the molecular diffusion coefficient D_v , that is, Schmidt number $Sc = \mu/\rho D_v$.

Even though no experimental data on axial dispersion have been published for supercritical fluids, we can approximate its effect as described below. For supercritical systems, the value of the Schmidt number, around 10, is intermediate to the values for gases ($Sc = 1.0$) and liquids ($Sc = 1000$). By comparing the order of magnitude of Schmidt number for gases, supercritical fluids and liquids, we can assume that the value of $P_{e,a}$ for SCF is so close to the value of $P_{e,a}$ for gas and is approximately equal to 2.0 when Re is greater than 1.0.

Kramers and Alberda⁴⁴ first discussed an analogy between a packed bed and a series of mixing vessels. By an analogy between the mechanism of imperfect mixing and Einstein's kinetic diffusion model, Carberry³⁷ showed that the number of perfect mixing tanks, n is given by:

$$n = \frac{Lu}{2\tau_a} = \frac{L}{d_p} \frac{P_{e,a}}{2} \quad (2-9)$$

As $E_a \rightarrow \infty$ for $n = 1.0$, then for a small number of mixers less than 10:⁴⁴

$$n - 1 = \frac{Lu}{2E_a} \quad (2-10)$$

These equations are used for determining the number of perfect mixers to be used in the cell model below.

Mass-Transfer Coefficient from the Cell Model

The cell model is a generalization of a class of models such as the completely mixed tanks-in-series model and the back-flow mixed tanks-in-series model. The common characteristic of this model is that the basic mixing unit is a completely mixed or stirred tank. This model has been employed extensively from early days of chemical engineering to the present.^{40,41,45-48} This cell model has the following practical advantages over other models:

1. The transition mixing behavior of such model can be presented by a set of linear first-order ordinary differential equations instead of partial differential equations.
2. The steady-state reaction in such a model can be represented by a set of finite difference equations rather than differential equations.

Since complete mixing is assumed in a cell, the mole fraction of a solute in out-going stream from the i th cell is y_i . If the bed is viewed as a series of n perfect mixing cells each having surface area of pellets A_T/n and constant mass-transfer coefficient k_y , then for the steady-state mass-transfer the material balance around the first cell gives

$$k_y(A_T/n)(y^* - y_1) = V_T(y_1 - y_0) \quad (2-11)$$

Finally, we can obtain the following expression for n cells by using the similarity for each cell (its derivation is not given here)

$$k_y a_S = \frac{nV_T}{SL_T} \left[\left(\frac{y^* - y_o}{y^* - y_n} \right)^{1/n} - 1 \right] \quad (2-12)$$

As mentioned above, we can assume that the value of $Pe_{e,a}$ for SCF is approximately equal to 2.0 when Re is greater than 1.0. Then, the number of perfect mixers in a packed bed can be determined by equation (2-9) or (2-10) depending upon the number of layers of the pellets in a packed bed (L/d_p). Finally, the mass-transfer coefficient under supercritical conditions can be obtained by equation (2-6) and/or (2-12) using the plug flow and/or cell models, respectively.

MASS-TRANSFER CORRELATIONS

After mass-transfer coefficients under supercritical conditions are determined, they need to be correlated as a function of the significant independent variables. Data on the rate of transfer between beds or particles and a flowing fluid are needed in the design of many industrial devices used for extraction, adsorption, leaching, ion exchange and chromatography. Numerous studies for packed beds have been carried out with the object of measuring mass-transfer coefficients and correlating the results under standard conditions, usually at 1 atm and 25°C. As far as we know, no data have been published on the mass-transfer coefficients under supercritical conditions. As several researchers pointed out,^{10,11} under supercritical conditions we expect correlations for mass-transfer coefficients to differ from those for mass-transfer coefficients of solid-gas or solid-liquid systems under standard conditions.

In general, mass-transfer between a fluid and a packed bed of solid can be described by correlations of the following form by the similarity to the

relationships obtained for heat transfer:

$$Sh = f(Re, Sc, Gr) \quad (2-13)$$

where Sh , Re , Sc , and Gr are respectively the Sherwood number, Reynolds, Schmidt, and Grashof numbers for the mass-transfer. Such a relationship has been obtained theoretically by Eckert⁴⁹ from a consideration of the boundary conditions.

Below we describe several existing correlations, developed under non-supercritical conditions, which may serve as guides for the correlations to be developed in this work.

Natural Convection

Recently, Debenedetti and Reid⁵⁰ pointed out that, in the case of supercritical fluids, buoyant effects had to be considered because supercritical fluids showed extremely small kinematic viscosities as a result of their high densities and low viscosities. The comparison of the properties of air, water, and mercury was given in Figure 2-8 to show the relative importance of buoyant forces at constant Reynolds number. From the last column in Figure 2-8, we can find that the effect of buoyant forces is more than two orders of magnitude higher in supercritical fluid than in normal liquids.

For transfer under natural convection condition, where the Reynolds number is unimportant, general expression reduces to

$$Sh = g(Sc, Gr) \quad (2-14)$$

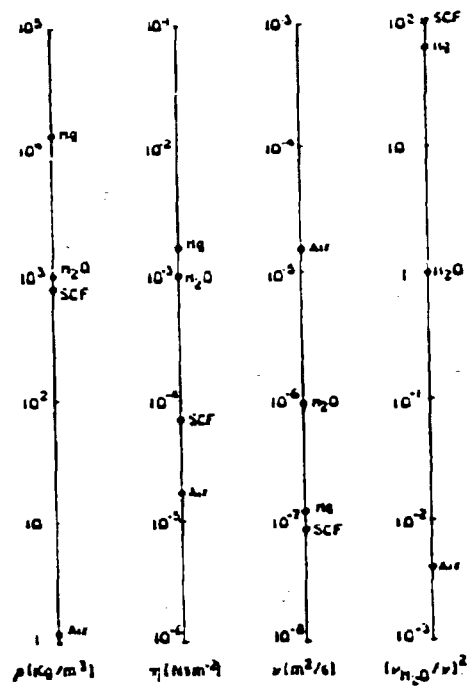


Figure 2-8: Comparison of physical properties of air, water, and mercury, and CO₂, showing relative importance of natural convection

at constant Reynolds numbers; air, H₂O, Hg at 298°K and 1 bar.

CO₂ at 310°K and 150 bar⁵⁰.

For large Schmidt number (usually liquid system) Karabeal et al.⁵¹ proposed the following typical form of relationship for this natural convection condition by the use of asymptotic relations.

$$Sh = 0.46(GrSc)^{1/4} \quad (2-15)$$

for laminar natural convection

$$Sh = 0.112(GrSc)^{1/3} \quad (2-16)$$

for turbulent natural convection.

If natural convection is dominant, the correlations like those above are likely to be appropriate for modeling the mass-transfer coefficient data. Its main difference is that it is independent of Reynolds number Re .

Forced Convection

Under forced convection conditions, where the Grashof number is unimportant, the general expression becomes

$$Sh = h(Re, Sc) \quad (2-17)$$

The most convenient method of correlating mass-transfer data under forced convection conditions is to plot the j_D factor as a function of Reynolds number as suggested by Colburn⁵ and Chilton and Colburn⁶ who, from theoretical consideration of flow and from dimensional analysis, defined j_D as follows:

$$j_d = \frac{Sh}{ReSc^{1/3}} = \frac{k_y M_{av}}{G} \left(\frac{\mu}{\rho D_v} \right)^{2/3} \quad (2-18)$$

In calculating the Schmidt number, $\mu/\rho D_v$, the viscosity and density of carbon dioxide will be used since the amount of naphthalene in carbon dioxide has a negligible effect on these properties.

The functional dependence of j_d on Reynolds number Re has been the subject of study by many investigators. A variety of equations have been proposed to represent their experimental data. Many of these correlations also employ the bed porosity ϵ as an additional correlating parameter. The porosity is the ratio of the void volume between pellets to the total bed volume. Two typical correlations for solid-gas and solid-liquid systems are as follows:

1. Solid - Gas System:⁵²

$$\epsilon j_d = 0.357 Re^{-0.359} \quad 3 < Re < 2000 \quad (2-19)$$

2. Solid-Liquid System:⁸

$$\epsilon j_d = 0.25 Re^{-0.31} \quad 55 < Re < 1500 \quad (2-20)$$

$$\epsilon j_d = 1.09 Re^{-2/3} \quad 0.0016 < Re < 55 \quad (2-21)$$

Other proposed correlations of mass-transfer data are shown in Table 2-4.⁵¹

Combined Natural and Forced Convection

In the intermediate region where natural and forced convection happen simultaneously, neither the Reynolds number nor the Grashof number can be neglected. Garner and Grafton⁵³ suggested that the transfers due to the two processes are simply additive. Karabelas et al.⁵¹ proposed the following

correlations using an asymptotic method which are shown in Figure 2-9.

$$Sh = \left[\{0.46(GrSc)^{1/4}\}^6 + \{4.58 pe^{1/3}\}^6 \right]^{1/6} \quad (2-22)$$

for 1 in, and 1/2 in, spheres ($GrSc < 1.31 \times 10^8$)

$$Sh = \left[\{0.112(GrSc)^{1/3}\}^2 + \{2.39 Re^{0.56} Sc^{1/3}\}^2 \right]^{1/2} \quad (2.23)$$

For 3 in, sphere ($GrSc = 3.2 \times 10^9$)

Table 2-4: Correlations of mass-transfer data ⁵¹

Reference	Type of packing	Correlation	Re	Sc
61	Spherical and cylindrical pellets	$j_d = 16.8Re^{-1}$	< 40	0.61-0.62
62	Same as above	$j_d = 0.989Re^{-0.41}$	≥ 350	~ 0.615
63	Granular solid	$j_d = 1.82Re^{-0.51}$	< 350	~ 1000
		$StSc^{0.6} = 0.45Re^{-0.36}$	< 10	
		$StSc^{0.6} = 0.20Re^{-0.36}$	> 50	
64	Spheres and cylinders	$j_d = 1.251Re_m^{-0.41}$	$Re_m > 620$	~ 0.61
		$j_d = 2.44Re_m^{-0.51}$	$Re_m < 620$	
65	Spherical and flake shaped particles	$j_d = 1.625Re^{-0.307}$	< 120	1200-1500
		$j_d = 0.687Re^{-0.227}$	> 120	
66	Porous spherical particles soaked in an aqueous solution	$\log j_d = 0.7683 - 0.915 \log Re + 0.0817 [\log Re]^2$	0-10,000	776 and 865
67	Pellets of succinic and salicylic acids	$StSc^{-0.36} = 1.97 \left[\frac{Re}{\epsilon} \right]^{-0.413}$	$\frac{Re}{\epsilon} < 200$	150-13,000
		$StSc^{-0.36} = 0.29 \left[\frac{Re}{\epsilon} \right]^{-0.254}$	$\frac{Re}{\epsilon} > 200$	
68	Various particle geometries	$j_d = \frac{150(1-\epsilon)}{6\epsilon} Re^{-1} Sc^{-1/3} + \frac{1.75}{6\epsilon} Sc^{-1/3}$	wide range	wide range
69	Spheres	$j_d = 1.46 \left[\frac{6G}{u\mu} \right]^{-0.41} (1-\epsilon)^{0.2}$	$\frac{6G}{u\mu} > 100$	wide range
		$j_d = 17 \left[\frac{6G}{u\mu} \right]^{-1} (1-\epsilon)^{0.2}$	$\frac{6G}{u\mu} < 10$	
70	Porous spheres	$j_d = 10Re^{-1}$	< 50	low
		$j_d = 1.30Re^{-0.42}$	> 150	
71	Benzoic acid granules	$j_d = 1.48Re^{-0.32}$	1-70	~ 1000
72	Various particle types	$j_d = 5.7 \left[\frac{Re}{1-\epsilon} \right]^{-0.76}$	$1 < \frac{Re}{1-\epsilon} < 30$	0.6-10,000
		$j_d = 1.77 \left[\frac{Re}{1-\epsilon} \right]^{-0.44}$	$30 < \frac{Re}{1-\epsilon} < 10^4$	
73	Spherical particles	$j_d = 0.667Re^{-0.24}$	20-200	
74	Porous spheres	$j_d = \frac{0.725}{Re^{0.41} - 1.5}$	13-2136	0.606
75	Fixed and fluidized beds of spheres	$\epsilon j_d = 0.010 + \frac{0.863}{Re^{0.36} - 0.483}$	> 1	wide range
75	Fixed and fluidized beds of particles with various geometries	$\frac{\epsilon j_d}{f} = \frac{0.30}{Re_m^{0.33} - 1.90}$	$Re_m > 50$	wide range
76	Spherical particles	$StSc^{0.36} = 2.40 \left[\frac{Re}{\epsilon} \right]^{-0.41}$	$0.08 < \frac{Re}{\epsilon} < 125$	~ 1000
		$StSc^{0.36} = 0.442 \left[\frac{Re}{\epsilon} \right]^{-0.31}$	$125 < \frac{Re}{\epsilon} < 5000$	
77	Porous spherical and cylindrical particles	$j_d = 2.25 \left[\frac{Gd}{\mu} \frac{1}{1-\epsilon} \right]^{-0.301}$	wide range	0.60

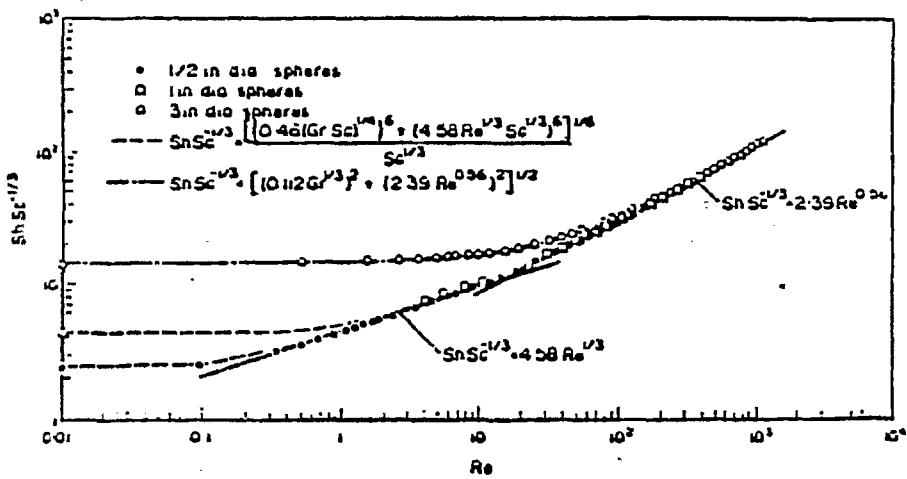


Figure 2-9: Asymptotic correlations for the combined natural and forced convection⁵¹

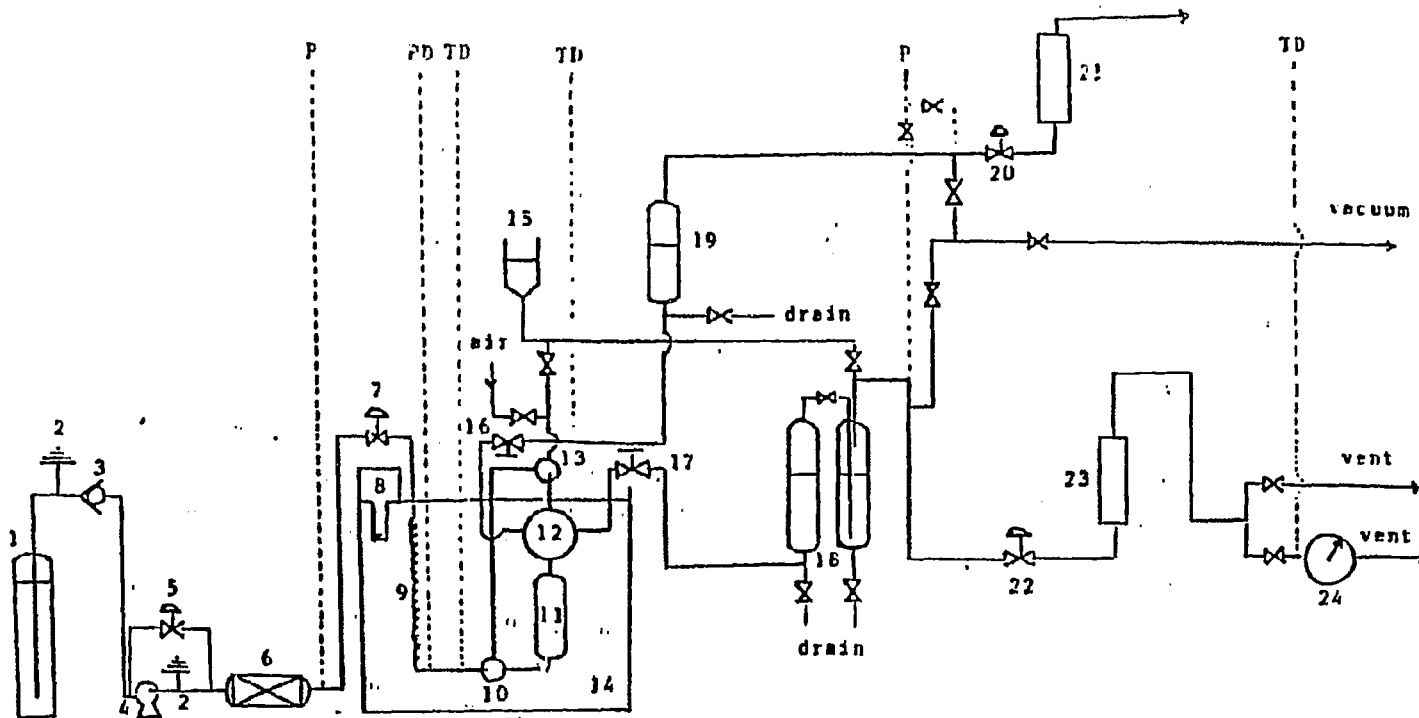
EXPERIMENTAL

The schematic diagram of the experimental apparatus used in this study is shown in Figure 2-10. Liquid carbon dioxide is pumped into the system via a high-pressure Milton-Roy liquid pump. Pressure is controlled by using a back pressure regulator and pressure fluctuation is dampened with an on-line surge tank. The system consists of a preheater which allows the solvent to reach the desired temperature and the extraction vessel 171 cm³ in volume, 14.6 cm in length and 3.87 in diameter. The extraction vessel is packed with naphthalene pellets which have been made from pure naphthalene using a die. The height of the packing in the bed can be changed by using inert packing at the bottom and the top of the bed. The inert packing material being used is glass beads with size similar to that of the pellets. Another advantage in using the inert pellets is to get rid of end effects in the packed bed being used as the extractor. Pressure at the inlet of extractor is measured using a pressure transducer. The temperature of the extractor is measured at the inlet.

The fluid mixture coming out of the extractor is depressurized to atmospheric pressure by passing it through a heated metering valve and a back pressure regulator. The instantaneous flow rate of the gas leaving the extractor is measured using a rotameter and the total amount of gas flow is measured with a calibrated wet-test meter.

The mass of precipitated solid is found as described below. With this value and total amount of gas flow through wet-test meter, the mole fraction of solids in the supercritical fluid can be readily determined. The temperature and pressure in wet-test meter are also measured.

The sample collectors are high pressure bombs which are kept at room temperature by two 200 watt resistance heaters. Each vessel contains toluene



- | | | |
|----------------------------|---------------------|-----------------------------|
| 1. Cylinder | 9. Preheater | 17. Metering valve |
| 2. Relief valve | 10. Three-way valve | 18. Sample tanks |
| 3. Check valve | 11. Extractor | 19. Solid trap |
| 4. Liquid pump | 12. Four-way valve | 20. Back pressure regulator |
| 5. Back pressure regulator | 13. Three-way valve | 21. Rotameter |
| 6. Surge tank | 14. Water bath | 22. Back pressure regulator |
| 7. Pressure regulator | 15. Solvent tank | 23. Rotameter |
| 8. Temperature controller | 16. Metering valve | 24. Wet test meter |

P: Pressure gauge
 PD: Pressure transmitter to Data logger
 TD: Thermocouple to Data logger

Figure 2-10: Schematic diagram of the experimental apparatus of SCFE

which will help dissolve the extract (naphthalene) from the carbon dioxide. These vessels are operated at 300 to 400 psi where the solubility of the solid in the carbon dioxide is at a minimum. The second vessel is redundant and is used to guarantee that all of the extract is collected and to reduce entrainment losses. No naphthalene was found in these vessels during current experiments. To determine the amount of extract collected, the amount of toluene (with dissolved extract) is weighed. A sample of the toluene-extract solution is then injected into a gas chromatograph to determine what portion of the solution is extract. Finally, the bypass, from valve 12 to 16, is designed to insure steady-state flow through the extraction vessel 11.

The whole apparatus is rated for a pressure of 5000 psi. All measured temperatures and pressures are recorded on a data logger at regular time intervals. The parameters that are being studied are:

- Effect of flow rate on solubility of naphthalene in carbon dioxide at different pressures and temperatures.
- Effect of bed height on the mass-transfer coefficient under supercritical conditions.
- Effect of flow rate on the mass-transfer coefficient under supercritical conditions.
- Effect of pressure on the mass-transfer coefficient under supercritical conditions.

The experimental conditions are as follows:

System: Naphthalene - Carbon Dioxide

Pellet Characteristics:

Material: Naphthalene

Shape: Cylindrical

Size: Length (mm) = 4.76
 Diameter (mm) = 4.76
Height of Bed (mm): 4.76 - 19.04
Temperature of Bed (°K): 308, 318, 328
Pressure (psi): 1470, 2205, 2940, 3675
Flow Rates (STD. liter/min at 0°C and 1 atm): 4 - 30
Reynolds Number: $10 < Re < 250$
Schmidt Number: $5 < Sc < 12$
Grashof Number: $1.69 \times 10^6 < Gr < 2.13 \times 10^7$

PLANS

This work is divided into two major parts. The first part is to measure mass-transfer coefficients, while the second one is concerned with establishing the mass-transfer correlations under supercritical conditions.

Mass-transfer coefficients in packed beds under standard conditions have been measured using various flow models. However, no study has yet been carried out to estimate the mass-transfer coefficient under supercritical conditions and no mass-transfer correlations under these conditions have been developed.

For this fundamental mass-transfer study under supercritical conditions, naphthalene-CO₂ systems have been chosen due to convenience of getting the values of transport properties such as binary diffusion coefficient, viscosity and density of carbon dioxide from the literature. Experiments are being carried out to investigate the effect of the flow rate of CO₂ on solubility of naphthalene in CO₂. The effect of flow rate on CO₂, temperature, and pressure on mass-transfer coefficients will be determined using the plug flow model and cell model. Then, these mass-transfer coefficient data will be used to develop mass-transfer

correlations analogous to those shown in the previous section which would be useful in designing separation units. Finally, these correlations for solid-supercritical fluid will be compared with mass-transfer correlations for solid-gas and/or solid-liquid systems, depending upon three different flow conditions, respectively (natural, forced, and combined natural and forced convection).

Results

Work for Current Period (April 1 - June 30)

In the schematic diagram of Figure 2-10 the sample tanks were replaced by new ones to get more accurate results by collecting all toluene including dissolved naphthalene in sample tanks.

After revising our system, we operated it continuously for 2 minutes at 35°C and 100 atm for several flow rates of carbon dioxide. The resultant data of mass transfer coefficients are obtained for different flow rate and are shown in Table 2-5.

In Figure 2-11, we showed the relationship between mass transfer coefficient k_g vs. mass velocity G . Figure 2-12 is a plot of mass transfer factor j_d vs. Reynolds number Re $Re = (\rho dp U_g)/\mu$. In both graphs, more dataa is needed to determine the true correlations. A wider range of the experimental conditions will be studied in the next two quarters.

TABLE 2-5

Results for Mass Transfer Coefficients and j_d vs. Re Correlations at 35°C and 100 atm

Run No.	Superficial Flow Rate (g/min) at 1 atm	Exit mole Fraction, $y \times 10^3$	Mass Velocity, G $\times 10^2$	Mass Transfer Coefficient, kg $\times 10^4$	Mass Transfer Factor j_d	Reynolds Number, Re
	24.158	3.0344	6.84	1.782	0.4393	55.77
	21.922	3.1736	6.21	1.725	0.4685	50.61
	19.324	3.4816	5.48	1.744	0.5373	44.61
	17.798	3.6258	5.05	1.710	0.5719	41.09
	15.8175	3.8852	4.49	1.695	0.6376	36.51
	14.009	4.3036	3.98	1.779	0.7553	32.34
	12.922	4.3182	3.67	1.652	0.7603	29.83
	10.906	4.8020	3.10	1.688	0.9201	25.18
	9.539	5.0142	2.72	1.605	0.9999	22.02
	7.815	5.5023	2.23	1.592	1.2099	18.04

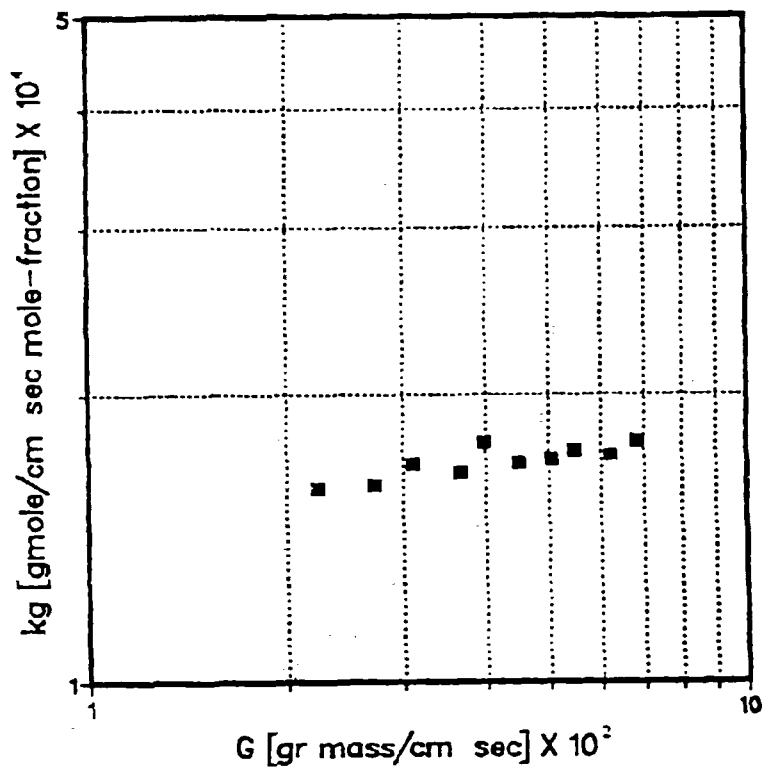


FIGURE 2-11: Correlation between kg and G at 35°C and 100 atm

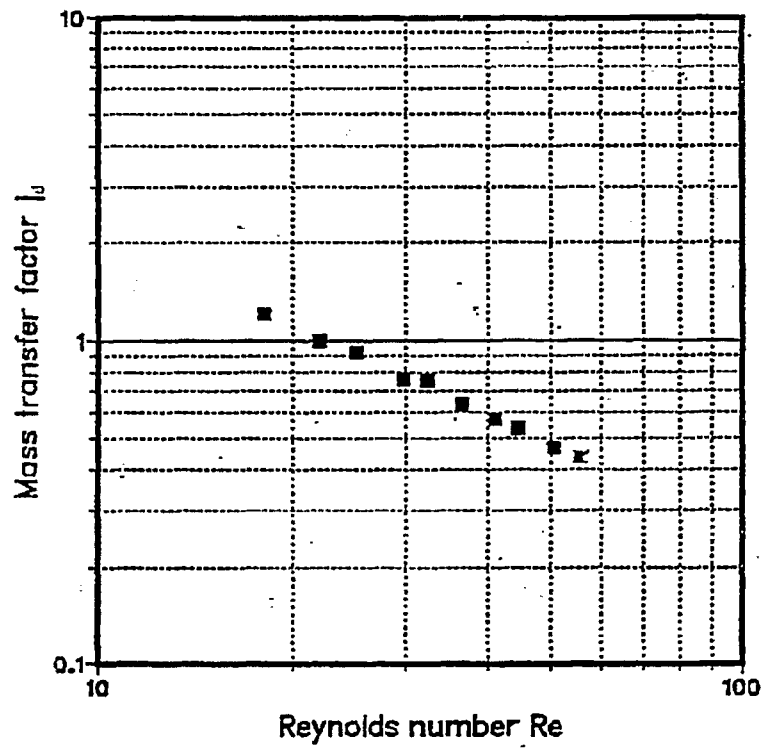


FIGURE 2-12: Relationship between i_d and Reynolds Number Re for Beds of Cylindrical Pellets at 35°C and 100 atm

Comparison of our data with those of ordinary systems such as CO₂(g)-naphthalene⁵⁴ and water-naphthalene⁵⁵ under standard conditions (usually 1 atm and 25°C) is shown in Figure 2-13. It shows that the mass-transfer rates under supercritical conditions were high (same order-of-magnitude as CO₂(g)-naphthalene system), and their numerical values lay in between those of solid-gas and solid-liquid as expected.

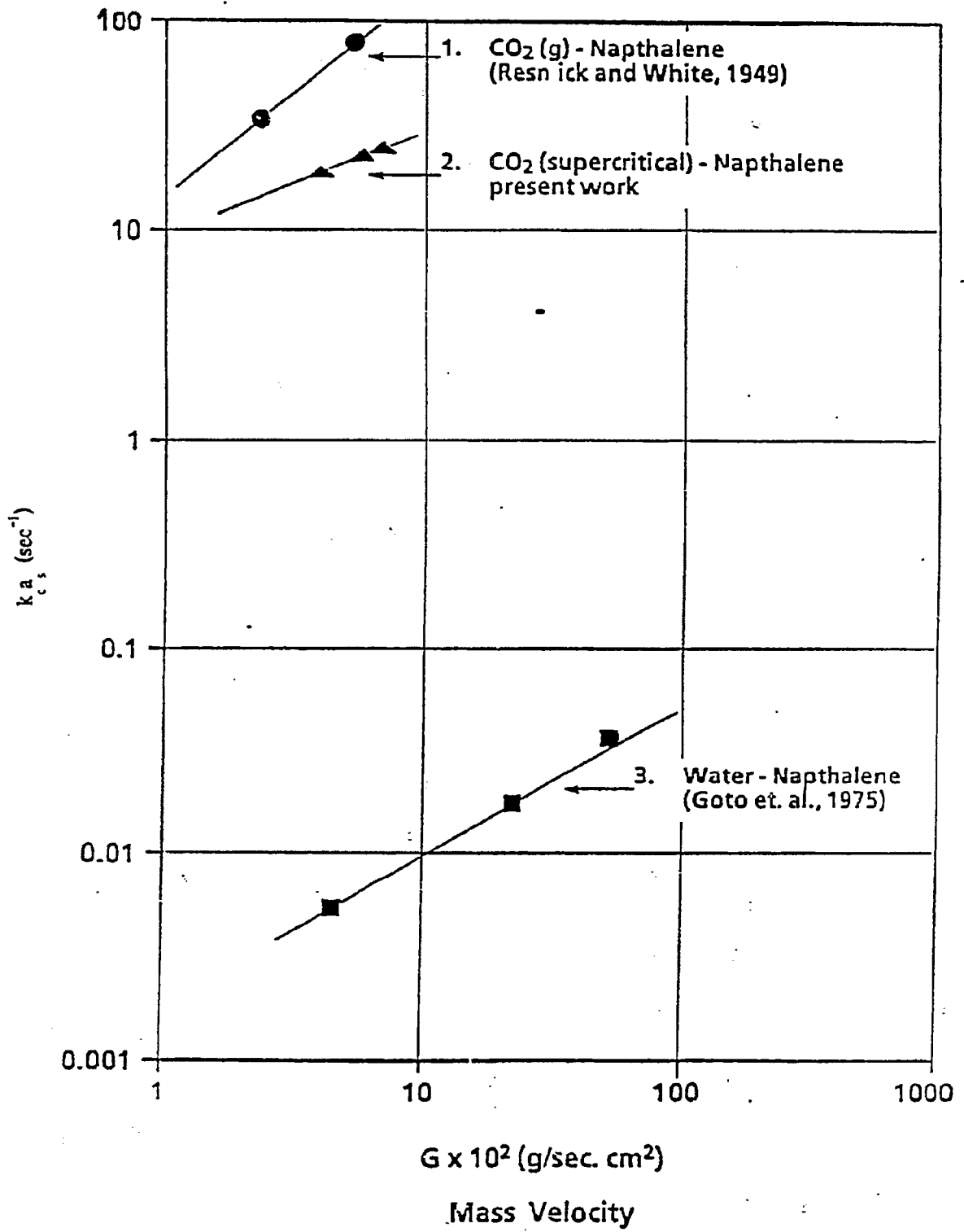


Figure 2-13: Comparison of supercritical condition with G-S and L-S system

NOMENCLATURE

a	:	System parameter in Peng-Robinson equation of state
a_S	:	Surface area of pellets per unit volume of extractor [cm^2/cm^3]
A_p	:	Surface area of single particle [cm^2]
A_T	:	Total surface area of pellets in extractor [cm^2]
b	:	System parameter in Peng-Robinson equation of state
C	:	Concentration of solute [gmole/cm^3]
d_p	:	Diameter of sphere possessing the same surface area as a piece of packing [cm]
D_v	:	Molecular diffusivity [cm^2/sec]
E_a	:	Axial dispersion coefficient [cm^2/sec]
E_r	:	Radial dispersion coefficient [cm^2/sec]
f_i^S	:	Fugacity of component i in solid phase [atm]
f_i^V	:	Fugacity of component i in vapor phase [atm]
g	:	Gravitational acceleration [cm/s]
G	:	Mass velocity [$\text{g}/\text{cm}^2\text{sec}$]
\bar{G}_{My}	:	Average molal mass velocity [$\text{gmole}/\text{cm}^2\text{sec}$]
G_{My}	:	Molal mass velocity [$\text{gmole}/\text{cm}^2\text{sec}$]
Gr	:	Grashof number = $d^3 g \rho \Delta \rho / \mu^2$
j_d	:	Mass transfer factor = $Sh Re^{-1} Sc^{-1/3}$
k_c	:	Mass transfer coefficient = $k_y C$ [cm/sec]
k_{ij}	:	Binary interaction parameter
k_y	:	Mass transfer coefficient [$\text{gmole}/\text{cm}^2\text{sec mole-fraction}$]
L_T	:	Total height of bed [cm]
M_{av}	:	Average molecular weight [g/gmole]

n	:	Number of perfect mixers
N_A	:	Molal flux of solute [gmole/cm ² sec]
P	:	Total pressure [atm]
P_c	:	Critical pressure [atm]
Pe	:	Peclet number = $u_s d_p / D_v$
$Pe_{e,a}$:	Axial peclet number = $u d_p / E_a$
P_i^s	:	Saturation (Vapor) pressure of pure solid [atm]
R	:	Gas constant = 0.08205 [atm liter/gmole °K]
Re	:	Reynolds number = $\rho d_p u_s / \mu$
S	:	Cross section area of packed bed [cm ²]
Sc	:	Schmidt number = $\mu / \rho D_v$
Sh	:	Sherwood number = $k_c d_p / D_v$
T	:	Absolute temperature
T_c	:	Critical temperature [°K]
T_r	:	Reduced temperature
T_ϵ	:	Tortuosity of bed
u	:	Interstitial velocity [cm/sec]
u_s	:	Superficial velocity [cm/sec]
V_T	:	Total molal flow rate [gmole/sec]
V	:	Molal flow rate of inert component [gmole/sec]
y_A	:	Mole fraction of component A
y_A^*	:	Equilibrium mole fraction of component of A
y_i	:	Mole fraction of component A in stream outgoing from ith cell
Z	:	Compressibility factor

Greek Letters

ϵ	:	Void fraction
ϕ_{iV}	:	Fugacity coefficient of component i in vapor phase
ϕ_{iS}^S	:	Fugacity coefficient of component i in solid phase at saturation pressure P_i^S
γ_i^∞	:	Activity coefficient at infinite dilution
μ	:	Viscosity [g/cm sec]
ρ	:	Density [g/cm ³]

BIBLIOGRAPHY

1. Chang, H. and Morrell, D.G., "Solubilities of Methoxy-1-Tetralone and Methyl Nitrobenzoate Isomers and their Mixtures in Supercritical Carbon Dioxid," *J. Chem. Eng. Data*, Vol. 30, 1985, pp.74.
2. Irani, C.A. and Funk, E.W., Separation Using Supercritical Gases, CRC Hand Book, CRC Press, Boca Raton, FL, 1977, pp. 171, Ch. Part A.
3. Paul, P.F.M. and Wise, W.S., The Properties of Gases Extraction, Mills and Boom Ltd., London, 1971.
4. Sirtl, W., "Examples of Cost Determinations," High Pressure Extraction Symposium, NOVA-WERKE AG. Effretikon, Switzerland, August 1979.
5. Colburn, A.P., "A Method of Correlating Forced Convection Heat Transfer Data and a Comparison with Fluid Friction," *AIChE J.*, Vol. 29, 1933, pp. 174.
6. Chilton, T.H. and Colburn, A.P., "Mass-Transfer (Absorption) Coefficients (Prediction from Data on Heat Transfer and Fluid Friction)," *Ind. Eng. Chem.*, Vol. 26, 1934, pp. 1183.
7. Gupta, A.S. and Thodos, G., "Mass and Heat Transfer in the Flow of Fluids through Fixed and Fluidized Beds of Spherical Particles," *AIChE J.*, Vol. 8, 1962, pp. 608.
8. Wilson, E.J. and Geankoplis, C.J., "Liquid Mass-Transfer at Very Low Reynolds Numbers in Packed Beds," *Ind. Eng. Chem. Fund.*, Vol. 5, 1966, pp. 9.
9. Storck, A. and Coeuret, F., "Mass-Transfer Between a Flowing Liquid and a Wall or an Immersed Surface in Fixed and Fluidized Beds," *Chem. Eng. J.*, Vol. 20, 1980, pp. 149.
10. Pfeffer, R., "Heat and Mass Transfer in Multiparticle Systems," *Ind. Eng. Chem. Fund.*, Vol. 3, 1964, pp. 380.
11. Bradshaw, R.D. and Bennett, C.O., "Fluid-Particle Mass Transfer in a Packed Bed," *AIChE J.*, Vol. 7, 1961, pp. 48.
12. Hannay, J.B., "On the Solubility of Solids in Gases," *Proc. Roy. Soc. (London)*, Vol. 30, 1880, pp. 484.
13. Hannay, J.B. and Hogarth, J., "On the Solubility of Solids in Gases," *Proc. Roy. Soc. (London)*, Vol. 29, 1879, pp. 324.
14. Hannay, J.B. and Hogarth, J., "On the Solubility of Solids in Gases," *Proc. Roy. Soc. (London)*, Vol. 30, 1880, pp. 178.
15. Buchner, E.H., "Flussige Kohlensaure als Losungsmittel," *Z. Physik. Chem.*, Vol. 54, 1906, pp.665.

16. Centnerszwer, M., "Uber Kritische Temperaturen der Losungen," Z. Physik. Chem., Vol. 46, 1903, pp. 427.
17. Sage, B.H., Webster, D.C. and Lacey, W.N., "Phase Equilibria in Hydrocarbon Systems: XVI. Solubility of Methane in Four Light Hydrocarbons," Ind. Eng. Chem., Vol. 28, 1936, pp. 1045.
18. Kay, W.B., "Liquid-Vapor Phase Equilibrium Relations in the Ethane-n-Heptane System," Ind. Eng. Chem., Vol. 30, 1938, pp. 459.
19. Messmore, H.E., U.S. Pat. 2,420,185, 1943.
20. Maddocks, R.R. and Gibson, "Supercritical Extraction of Coal," J. Chem. Eng. Progr., Vol. 73, 1977, pp. 59.
21. Tugrul, T. and Oclay, A., "Supercritical Gas Extraction of Two Lignites," Fuel, Vol. 57, 1978, pp. 415.
22. Bartle, K.D. et al., "Chemical Nature of a Supercritical-Gas Extract of Coal at 350°C," Fuel, Vol. 54, 1975, pp. 227.
23. Barton, P. and Fenske, M.R., "Hydrocarbon Extraction of Saline Water," Ind. Eng. Chem. Process Des., Vol. 9, 1970, pp. 18.
24. Hubert, P. and Vitzhum, O., "Fluid Extraction of Hops, Spices and Tobacco with Supercritical Gases," Agnew Chem. Inc., Vol. 17, 1978, pp. 710, England.
25. Modell, M., deFelippi, R.P. and Krukonis, V., "Regeneration of Activated Carbon with Supercritical Carbon Dioxide," Am. Chem. Soc. Meet., Miami, September 1978.
26. Modell, M. et al., "Supercritical Fluid Regeneration of Activated Carbon," 87th Nat. Meet. Am. Inst. Chem. Eng., 1979.
27. Diepen, G.A.M. and Scheffer, F.E.C., "The Solubility of Naphthalene in Supercritical Ethylene II," J. Phys. Chem., Vol. 57, 1953, pp. 575.
28. Tsekhanskaya, Yu., V., Iomtev, M.B. and Mushkina, E.V., "Solubility of Naphthalene in Ethylene and Carbon Dioxide under Pressure," Russ. J. Phys. Chem., Vol. 38, 1964, pp. 1173.
29. Modell, M. et al., " ", 72nd AIChE J. Annual Meeting, San Francisco, CA, Nov., 1979.
30. Mackay, M.E. and Paulaitis, M.E., "Solid Solubilities of Heavy Hydrocarbons in Supercritical Solvents," Ind. Chem. Fund., Vol. 18, 1979, pp. 149.
31. Peng, D.Y. and Robinson, D.B., "A New Two-Constant Equation of State," Ind. Eng. Chem. Fund., Vol. 15, 1976, pp. 59.

32. Balenovic, Z., Myer, M.N., Giddings, J.E., "Binary Diffusion in Dense Gases to 1360 atm by Chromatographic Peak-Broadening Method," *J. Chem. Phys.*, Vol. 52, 1970, pp. 915.
33. Feist, R. and Schneider, G.M., "Determination of Binary Diffusion Coefficient of Benzene, Phenol, Naphthalene and Caffeine in Supercritical CO₂ between 308 and 333 °K in the Pressure Range 80 to 160 Bar with Supercritical Fluid Chromatography (SFC)," *J. Separation Sci. and Tech.*, Vol. 17, 1982, pp. 261.
34. Waid, I. and Schneider, G.M., "Determination of Binary Diffusion Coefficients of the Benzene and Some Alkylbenzenes in Supercritical CO₂ between 308 and 320°K in the Pressure Range 80 to 160 Bar with Supercritical Fluid Chromatography," *Ber Bunsenges. Phys. Chem.*, Vol. 83, 1979, pp. 969.
35. Paulaitis, M.E., Krukonis, V.J., "Supercritical Fluid Extraction," *Rev. Chem. Eng.*, Vol. 1, 1983, pp. 179.
36. Stephen, K. and Lucas, K., Viscosity of Dense Gas, Plenum Press, NY, 1979.
37. Carberry, J.J. and Bretton, R.H., "Axial Dispersion of Mass in Flow through Fixed Beds," *AIChE J.*, Vol. 4, 1958, pp. 367.
38. Chung, S.F. and Wen, C.Y., "Longitudinal Dispersion of Liquid Flowing through Fixed and Fluidized Beds," *AIChE J.*, Vol. 14, 1968, pp. 857.
39. Ebach, E.A. and White, R.R., "Mixing of Fluids Flowing through Beds of Packed Solids," *AIChE J.*, Vol. 4, 1958, pp. 161.
40. Cholette, A. and Cloufier, L., " ", *Can. J. Chem. Eng.*, Vol. 37, 1959, pp. 105.
41. Danckwerts, P.V., "Continuous Flow System (Distribution of Residence Time)," *Chem. Eng. Sci.*, Vol. 2, 1953, pp. 1.
42. Wen, C.Y. and Fan, L.T., Models for Flow Systems and Chemical Reactors, Marcel Dekker, Inc., NY, 1975.
43. Sherwood, T.K. et al., Mass-Transfer, McGraw-Hill Inc., NY, 1975, pp. 136.
44. Kramers, H. and Alberda, G., "Frequency Response Analysis of Continuous Flow Systems," *Chem. Eng. Sci.*, Vol. 2, 1953, pp. 173.
45. Adler, R.J. and Hovorka, R.B., " ", *JACC*, Denver, 1961.
46. Deans, H.A. and Lapidus, L., "A Computational Model for Predicting and Correlating the Behavior of Fixed Bed Reactor: 1. Derivation of Model for Non-Reactive Systems," *AIChE J.*, Vol. 6, 1960, pp. 656.
47. Levenspiel, O., "Mixed Models to Represent Flow of Fluids through Vessels," *Can. J. Chem. Eng.*, Vol. 40, 1962, pp. 135.

48. Levenspiel, O., Chemical Reaction Engineering, John Wiley and Sons, NY, 1962.
49. Eckert E.R.G., Introduction to Heat and Mass Transfer, McGraw-Hill Inc., NY, 1950.
50. Debenedetti, P.G. and R.C. Reid, "Diffusion and Mass-Transfer in Supercritical Fluids," *AIChE J.*, Vol. 32, 1986, pp. 2034.
51. Karabelas, A.J. et al., "Use of Asymptotic Relations to Correlate Mass-Transfer Data in Packed Beds," *Chem. Eng. Sci.*, Vol. 26, 1971, pp. 1581.
52. Petrovic, L.J. and Thodos, G., "Mass-Transfer in the Flow of Gases through Packed Bed," *Ind. Chem. Fund.*, Vol. 7, 1968, pp. 274.
53. Garner, F.H. and Grafton, R.W., " ", *Proc. Roy. Soc. (London)*, Vol. A224, 1954, pp. 64.
54. McHugh, M. and Paulaitis, M.E., "Solid Solubilities of Naphthalene and Biphenyl in Supercritical Carbon Dioxide," *J. Chem. Eng. Data*, Vol. 25, 1980, pp. 326.
55. Goto, S. et al., "Mass Transfer in Packed Beds with Two-Phase Flow," *Ind. Eng. Process Des. Dev.*, Vol. 14, 1975, pp. 473.
56. Morozov, V.S. and Vinkler, E.G., "Measurement of Diffusion Coefficients of Vapors of Solids in Compressed Gases. I. Dynamic Method for Measurement of Diffusion Coefficients," *Russ. J. Phys. Chem.*, Vol. 49, 1975, pp. 1404.
57. Vinkler, E.G. and Morozov, V.S., "Measurement of Diffusion Coefficients of Vapors in Compressed Gases. II. Diffusion Coefficients of Naphthalene in Nitrogen and In Carbon Dioixde," *Russ. J. Phys. Chem.*, Vol. 49, 1975, pp. 1405.
58. Iomtev, M.B. and Tsekhanskaya, Yu. V., "Diffusion of Naphthalene in Compressed Ethylene and Carbon Dioxide," *Russ. J. Phys. Chem.*, Vol. 38, 1964, pp. 485.
59. Tsekhanskaya, Yu. V., "Diffusion in the System p-Nitrophenol-Water in the Critical Region," *Russ. J. Phys. Chem.*, Vol. 42, 1968, pp. 532.
60. Schneider, G.M., "Chem. Thermodynamics Specialists Periodical Report," *Tech. Report, Chem. Soc., London*, 1978, Vol. 2, Chap. 4.
61. Gamson, B.W. et al., "Heat, Mass and Momemtum Transfer in the Flow of Gases through Granular Solids," *AIChE J.*, Vol. 39, 1943, pp. 1.

SATISFACTION GUARANTEED

NTIS strives to provide quality products, reliable service, and fast delivery. Please contact us for a replacement within 30 days if the item you receive is defective or if we have made an error in filling your order.

- ▶ **E-mail: info@ntis.gov**
- ▶ **Phone: 1-888-584-8332 or (703)605-6050**

Reproduced by NTIS

National Technical Information Service
Springfield, VA 22161

This report was printed specifically for your order from nearly 3 million titles available in our collection.

For economy and efficiency, NTIS does not maintain stock of its vast collection of technical reports. Rather, most documents are custom reproduced for each order. Documents that are not in electronic format are reproduced from master archival copies and are the best possible reproductions available.

Occasionally, older master materials may reproduce portions of documents that are not fully legible. If you have questions concerning this document or any order you have placed with NTIS, please call our Customer Service Department at (703) 605-6050.

About NTIS

NTIS collects scientific, technical, engineering, and related business information – then organizes, maintains, and disseminates that information in a variety of formats – including electronic download, online access, CD-ROM, magnetic tape, diskette, multimedia, microfiche and paper.

The NTIS collection of nearly 3 million titles includes reports describing research conducted or sponsored by federal agencies and their contractors; statistical and business information; U.S. military publications; multimedia training products; computer software and electronic databases developed by federal agencies; and technical reports prepared by research organizations worldwide.

For more information about NTIS, visit our Web site at <http://www.ntis.gov>.

NTIS

**Ensuring Permanent, Easy Access to
U.S. Government Information Assets**



U.S. DEPARTMENT OF COMMERCE
Technology Administration
National Technical Information Service
Springfield, VA 22161 (703) 605-6000
